On the Resolution of Approximation Errors on an Ensemble of Numerical Solutions

Alekseev A.K.[0000-0001-8317-8688], Bondarev A.E.[0000-0003-3681-5212]

Keldysh Institute of Applied Mathematics RAS, Moscow, Russia

aleksey.k.alekseev@gmail.com, bond@keldysh.ru

Abstract. Estimation of approximation errors on an ensemble of numerical solutions obtained by independent algorithms is addressed in the linear and nonlinear cases. In linear case the influence of the irremovable uncertainty on error estimates is considered. In nonlinear case, the nonuniform improvement of estimates' accuracy is demonstrated that enables to overperform the quality of linear estimates. An ensemble of numerical results, obtained by four OpenFOAM solvers for the inviscid compressible flow with an oblique shock wave, is used as the input data. A comparison of approximation errors, obtained by these methods, and the exact error, computed as the difference of numerical solutions and the analytical solution, is presented. The numerical tests demonstrated feasibility to obtain the reliable error estimates (in the linear case) and to improve the accuracy of certain approximation error in the nonlinear case.

Keywords: approximation error, ensemble of numerical solutions, irremovable uncertainty, Euler equations, OpenFOAM.

1 Introduction

The development of the verification methods (*a posteriori* error estimation) is complicated by the formation of discontinuities for CFD problems, governed by equations of hyperbolic or mixed types. By this reason the corresponding progress is less considerable if compare with the finite element domain (elliptic equations) [1-3]. Nevertheless, modern CFD standards [9,10] require a verification of numerical solution. At present, the set of methods, such as defect correction [4] and Richardson extrapolation [5-8], are used for the approximation error estimation in CFD. Their recommendations are mainly based on the grid convergence in the form of the Richardson extrapolation or the Runge approach (which considers the solution on a fine grid as true one). However, the common methods of *a posteriori error* estimation in CFD have significant troubles. The defect correction is an intrusive method (it requires the modification of the code) and is based on some linearization and assumption of the smallness of error, which may violate at the strong shock waves. The Richardson extrapolation is not intrusive (based on postprocessing), but, unfortunately, requires several consequent refinements of the grid that cause high computational expenses.

ICCS Camera Ready Version 2023
To cite this paper please use the final published version:
DOI: 10.1007/978-3-031-36030-5_51

By these reasons, papers [8,11-13] consider nonintrusive methods of the pointwise error estimation, which do not require the mesh refinement. The need for at least three independent solvers and a relatively small accuracy of error estimates are their drawbacks.

The present paper considers the conditions that improve the accuracy of error estimates for the linear method [8,11,12]. Some properties of the nonlinear method [13] are discussed, which increase the accuracy for certain solution at the expense of the accuracy of others. The considered nonlinear version of the algorithm enables to estimate the approximation error with higher accuracy, if compare with the linear case.

2 The linear problem for the approximation error estimation using the differences of numerical solutions

An ensemble of n numerical solutions $u_m^{(i)}$ $(i = 1...n)$, computed on the same grid by different numerical algorithms contains some information regarding their approximation errors. Herein u is the gas-dynamics variables, i is the number of algorithm, m is the index ($m = 1,...,L$), marking the grid node in a vectorized form. Papers [8, 11, 12] address the estimation of the approximation errors on the ensemble of numerical solutions. The Inverse Problem, posed in the variational statement with the zero order Tikhonov regularization, is used to treat the differences between the solutions in these papers. The paper [13] applies the Inverse Problem for the nonlinear statement of approximation error estimation in the context of regularization.

Herein, we address estimation of the approximation errors on the ensemble of numerical solutions using several approaches. Some important features of the both linear and nonlinear formulations are considered, including non-uniform resolution of errors.

We start from the linear statement, based on differences of solutions. We denote the projection of the exact solution $\tilde{u}$ onto the grid as $\tilde{u}_m$ and the approximation error for $i-th$ solution as $\Delta u_m^{(i)} = u_m^{(i)} - \tilde{u}_m$. The point-wise differences of the numerical solutions $d_{ij,m} = u_m^{(i)} - u_m^{(j)} = \tilde{u}_{h,m} + \Delta u_m^{(i)} - \tilde{u}_{h,m} - \Delta u_m^{(j)} = \Delta u_m^{(i)} - \Delta u_m^{(j)}$ are computable and depend on approximation errors. The following relation can be stated:

$$D_{kj} \Delta u_m^{(j)} = f_{k,m} . \tag{1}$$

Herein, $f_{k,m}$ is a vectorized form of the differences of solutions, D_{kj} is a rectangular $N \times n$ matrix, the summation over a repeating index is implied (no summation over m). Since the relation $N = n \cdot (n-1)/2$ (N is the number of equations and RHS

ICCS Camera Ready Version 2023
To cite this paper please use the final published version:
DOI: 10.1007/978-3-031-36030-5_51

terms) is valid, the simplest case when the number of equations is equal the number of unknowns corresponds to the ensemble of three numerical solutions:

$$\begin{pmatrix} 1 & -1 & 0 \\ 1 & 0 & -1 \\ 0 & 1 & -1 \end{pmatrix} \begin{pmatrix} \Delta u_m^{(1)} \\ \Delta u_m^{(2)} \\ \Delta u_m^{(3)} \end{pmatrix} = \begin{pmatrix} u_m^{(1)} - u_m^{(2)} \\ u_m^{(1)} - u_m^{(3)} \\ u_m^{(2)} - u_m^{(3)} \end{pmatrix}. \quad (2)$$

At $n = 3$, the number of unknowns is equal to the number of data elements, at $n > 3$ it is greater. Unfortunately, the matrix inversion is infeasible at any n. It is caused by the invariance of the difference of solutions to a shift transformation: $u_m^{(j)} = \tilde{u}_m^{(j)} + b + \Delta u_m^{(j)}$ and $\Delta u_m^{(j)} = \Delta \tilde{u}_m^{(j)} + b$ for any $b \in (-\infty, \infty)$, where $\Delta \tilde{u}_m^{(j)}$ is the true error. By this reason, the problem (1) is underdetermined (non-unique).

An addition of linear terms containing solutions (without differences) to RHS can not remove the degeneracy, since the relation $u_m^{(j)} = \tilde{u}_m + b + \Delta \tilde{u}_m^{(j)} - b$ holds. Fortunately, the shift invariance is a purely linear effect. So, a transition to the nonlinear statement may cure this degeneration.

3 The nonlinear statements for the estimation of the approximation error

The paper [13] consider the opportunities, presented by the quasilinear (regarding the parameters of interest) equation $A(\vec{x})\vec{x} = f$, $\vec{x}_m = \{\Delta u_m^{(1)}, \Delta u_m^{(2)}, \Delta u_m^{(3)}, \tilde{u}_m)$ having the form:

$$\begin{pmatrix} 2u_m^{(1)} - \Delta u_m^{(1)} & 0 & 0 & u_m^{(1)} - \Delta u_m^{(1)} \\ 1 & 0 & -1 & 0 \\ 0 & 1 & -1 & 0 \\ 1/3 & 1/3 & 1/3 & 1 \end{pmatrix} \cdot \begin{pmatrix} \Delta u_m^{(1)} \\ \Delta u_m^{(2)} \\ \Delta u_m^{(3)} \\ \tilde{u}_m \end{pmatrix} = \begin{pmatrix} (u_m^{(1)})^2 \\ u_m^{(1)} - u_m^{(3)} \\ u_m^{(2)} - u_m^{(3)} \\ (u_m^{(1)} + u_m^{(2)} + u_m^{(3)})/3 \end{pmatrix}. \quad (3)$$

The Equation (3) contains the nonlinear term $(u_m^{(1)})^2$ at right hand side, which prohibit the shift invariance $u_m^{(j)} = \tilde{u}_m + \Delta u_m^{(j)} + b$.

The determinant of matrix A of Eq. (3) is equal $u_m^{(1)}$. So, this equation may be solved by the simple matrix inversion (for non-zero solutions). In order to account for the nonlinearity, the linearization of the following form $A(\vec{x}^q)\vec{x}^{q+1} = f$ can be used at the iterative solution of Eq. (3) (q is the number of iteration).

ICCS Camera Ready Version 2023
To cite this paper please use the final published version:
DOI: 10.1007/978-3-031-36030-5_51

Another nonlinear option (without differences of solutions) has the appearance:

$$\begin{pmatrix} 1 & 0 & 0 & 1 \\ 0 & 1 & 0 & 1 \\ 0 & 0 & 1 & 1 \\ 2u_m^{(1)} - \Delta u_m^{(1)} & 0 & 0 & u_m^{(1)} - \Delta u_m^{(1)} \end{pmatrix} \cdot \begin{pmatrix} \Delta u_m^{(1)} \\ \Delta u_m^{(2)} \\ \Delta u_m^{(3)} \\ \tilde{u}_m \end{pmatrix} = \begin{pmatrix} u_m^{(1)} \\ u_m^{(2)} \\ u_m^{(3)} \\ (u_m^{(1)})^2 \end{pmatrix}. \tag{4}$$

It may be directly checked that $\det A(x) = -u_m^{(1)}$ and this matrix also can be inverted, and the result of the inversion has the form:

$$A^{-1}(x) = \begin{pmatrix} -1 + \Delta u_m^{(1)} / u_m^{(1)} & 0 & 0 & 1/u_m^{(1)} \\ -2 + \Delta u_m^{(1)} / u_m^{(1)} & 1 & 0 & 1/u_m^{(1)} \\ -2 + \Delta u_m^{(1)} / u_m^{(1)} & 0 & 1 & 1/u_m^{(1)} \\ 2 - \Delta u_m^{(1)} / u_m^{(1)} & 0 & 0 & -1/u_m^{(1)} \end{pmatrix}. \tag{5}$$

The matrix $A(x)$ may be decomposed into a sum the known matrix and a disturbance, which depends on the unknown approximation error $A(x) = A + \Delta A$.

$$A(x) = \begin{pmatrix} 1 & 0 & 0 & 1 \\ 0 & 1 & 0 & 1 \\ 0 & 0 & 1 & 1 \\ 2u_m^{(1)} & 0 & 0 & u_m^{(1)} \end{pmatrix} + \begin{pmatrix} 0 & 0 & 0 & 0 \\ 0 & 0 & 0 & 0 \\ 0 & 0 & 0 & 0 \\ -\Delta u_m^{(1)} & 0 & 0 & -\Delta u_m^{(1)} \end{pmatrix}. \tag{6}$$

The matrix A may be applied to solve approximately the problem.

4 The numerical algorithms

In order to solve Eqs. (2), (3), (4) we apply three different numerical methods. The coincidence of results ensures the reliability of analysis. In order to solve Equations (3), (4) we apply the matrix inversion (Gauss-Jordan elimination) [14]. The matrix inversion may be implemented for non degenerated square matrices only. In order to solve degenerate equation (2) we apply the variational statement and the Moore-Penrose pseudoinverse [15,16] . The Moore-Penrose pseudoinverse for the degenerated matrices applies the regularization and has an appearance $A^+ = (A^* A + \alpha E)^{-1} A^*$. Herein A_{ij} may be rectangular, $i \geq j$ (j - number of unknowns, i - number of equations and RHS terms). The following index form was used for the Moore-Penrose pseudoinverse

ICCS Camera Ready Version 2023
To cite this paper please use the final published version:
DOI: 10.1007/978-3-031-36030-5_51

$$u_k = (A_{nj} \cdot A_{nk})^{-1} A_{ij} f_{i,m} = A_{ki}^{+} f_i , \quad A_{ki}^{+} = (A_{nj} \cdot A_{nk})^{-1} A_{ij} . \tag{7}$$

In order to obtain the steady and bounded solution of Equation (2) we also use the variational statement of the Inverse Problem that includes the zero order Tikhonov regularization [17,18]. In this statement the minimization of the functional is applied:

$$\varepsilon_m(\Delta\vec{u}) = 1/2(D_{ij}\Delta u_m^{(j)} - f_{i,m}) \cdot (D_{ik}\Delta u_m^{(k)} - f_{i,m}) + \alpha/2(\Delta u_m^{(j)} \Delta u_m^{(j)}) , \tag{8}$$

where α is the regularization parameter. The steepest gradient descent is applied for the search of minimum of the functional.

The minimum of the regularizing term enables to obtain solutions with the minimum shift error, since:

$$\min_{b_m} \sum_j^n (\Delta u_m^{(j)})^2 / 2 = \min_{b_m} (\delta(b_m)) = \min_{b_m} \sum_j^n (\Delta\tilde{u}_m^{(j)} + b_m)^2 / 2 . \tag{9}$$

The variation of the regularizing term over shift change may be stated as

$$\Delta\delta(b_m) = \sum_j^n (\Delta\tilde{u}_m^{(j)} + b_m)\Delta b_m . \tag{10}$$

So, its extremum occurs at:

$$b_m = -\frac{1}{n} \sum_j^n \Delta\tilde{u}_m^{(j)} = -\Delta\bar{u}_m . \tag{11}$$

Thus, the shift b_m is equal to the mean true error (with the opposite sign). By this reason, in linear approach (2), the error estimate $\left|\Delta u_m^{(j)}\right|$ cannot be less than $\left|b_m\right|$ and contains some irremovable uncertainty.

Formally, the presence of an irremovable uncertainty b_m is the main drawback of linear approach. Nevertheless, if errors magnitudes differ significantly (one is much greater others), then

$$b_m = -\frac{1}{n} \sum_j^n \Delta\tilde{u}_m^{(j)} \sim \Delta\tilde{u}_m^{(\max)} / n \tag{12}$$

and the irremovable uncertainty of greatest error is moderate, while the irremovable fault of small errors may be great. So, some errors (great) may be estimated enough

ICCS Camera Ready Version 2023
To cite this paper please use the final published version:
DOI: 10.1007/978-3-031-36030-5_51

accurately. Really, the numerical tests demonstrate the good resolution of great errors and the poor resolution of small errors.

The variational statement of problems (3) and (4) corresponds to the minimum of the following functional:

$$\varepsilon_m(\vec{x}_m) = 1/2(A^m_{ij}x^{(j)}_m - f_{i,m})\cdot(A^m_{ik}x^{(k)}_m - f_{i,m}) + \alpha/2(x^{(j)}_m x^{(j)}_m), \tag{13}$$

where $\vec{x}_m = \{\Delta u^{(1)}_m, \Delta u^{(2)}_m, \Delta u^{(3)}_m, \tilde{u}_m\}$. The dependence of the matrix A^m_{ij} on flow parameters is specific for this statement. The component of the solution $\tilde{u}_m$ does not suffer from the shift invariance, so the irremovable uncertainty is the same as in the linear case.

5 The test problem

The flowfield engendered by the oblique shock waves governed by two dimensional compressible Euler equations is used in the tests due to the availability of analytic solutions and the high level of the approximation errors. The flowfield is engendered by a plate at the angle of attack α = 20° in the uniform supersonic flow (M=4). The analytic solution is engendered by the Rankine-Hugoniot relations. The projection of the analytic solution on the computational grid is considered as a true solution and used for estimation of the true error.

The conditions at the left boundary ("*inlet*") and at the upper boundary *("top")* are specified by the inflow parameters. The conditions at the right boundary ("*outlet*") are specified by the zero gradient condition. The conditions at the down boundary, which ensure the non-penetration on the plate surface, are posed by the zero normal gradient for the pressure and the temperature and the "*slip*" condition for the speed.

The following solvers are used that belong to the OpenFOAM software package [19]:

- *rhoCentralFoam* (rCF), based on the central-upwind scheme [20,21].
- *sonicFoam* (sF), based on the PISO algorithm [22].
- *pisoCentralFoam* (pCF) [23], which combines the Kurganov-Tadmor scheme [20] and the PISO algorithm [22].
- *QGDFoam (QGDF),* which implements the quasi-gas dynamic algorithm [24].

6 Numerical results

The numerical results for error analysis are provided in Figures 1-8 for $\alpha = 20^o, M = 4$. The index along the abscissa axis $i = N_y(k_x - 1) + m_y$ is defined by indexes along X (k_x) and Y (m_y). The jump of variables corresponds to the shock wave. The magnitudes of the numerical and analytical density are provided.

ICCS Camera Ready Version 2023
To cite this paper please use the final published version:
DOI: 10.1007/978-3-031-36030-5_51

The Figures present also the true density error $\Delta\rho_m^{(i)} = \rho_m^{(i)} - \tilde{\rho}_m$, the error estimates using linear (2) and nonlinear (3), (4) approaches (practically coinciding in tests), and the irremovable uncertainty $b_m = -\frac{1}{n}\sum_{j}^{n} \Delta\tilde{\rho}_m^{(j)}$.

First, the ensemble of rCF,pCF,sF solvers is used. The Fig. 1 presents the vectorized density and estimates of error for the solution computed by rCF method. The numerical solution, the analytical solution, true error $\Delta u_m^{(i)} = u_m^{(i)} - \tilde{u}_m$, the irremovable uncertainty, the linear (Eq. (2)), and nonlinear estimates of error (Eq. (4)) are presented.

The Fig. 2 presents the analogical information for rCF based solution, Fig. 3 demonstrates the information regarding sF based solution.

The Fig. 1 and Fig. 2 present the cases when the irremovable uncertainty is close to the true error. One may see the relative poor quality of the linear error estimation for these cases. The Fig. 3 presents the case when the irremovable uncertainty is lesser the true error and it is unable to spoilt the estimates.

The nonlinear estimates for the case of Fig. 1 are zero, so they are not presented. In Fig. 2 they are close to zero and nonrealistic. The nonlinear estimate (Eq. (4)) presented in Fig. 3 is close to the true error and overperforms the linear estimate (Eq. (2)). One can see that the nonlinear estimates (Eq. (4)) have significant anisotropy of sensitivity.

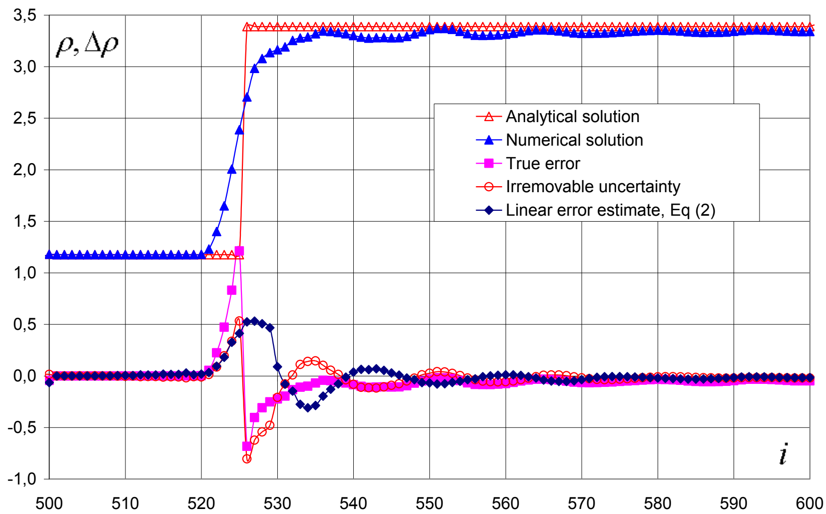

Fig. 1. The vectorized density and density errors for solution computed by rCF solver.

ICCS Camera Ready Version 2023
To cite this paper please use the final published version:
DOI: 10.1007/978-3-031-36030-5_51

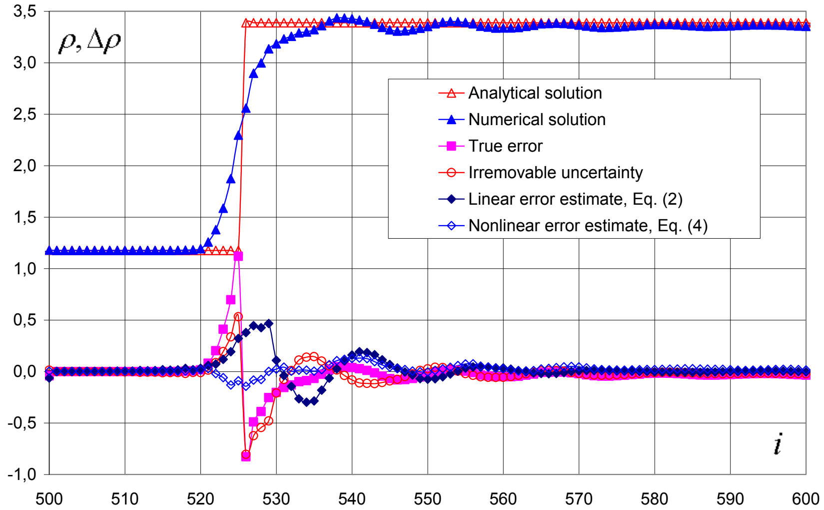

Fig. 2. The vectorized density and density errors for solution computed by pCF solver.

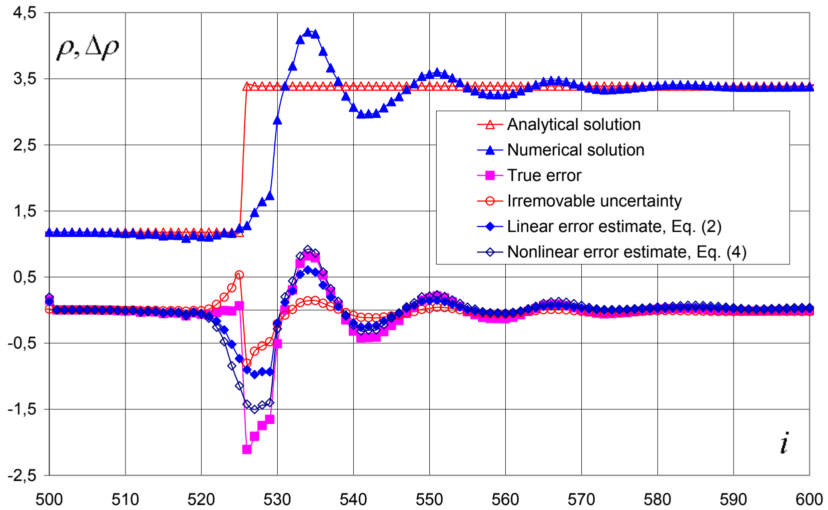

Fig. 3. The vectorized density and density errors for solution computed by sF solver.

The largest approximation error (specific for sF algorithm) is resolved with the best quality. It is interesting that the quality depends on the choice of the algorithm. Figs. 1-3 demonstrate the dependence of the quality on the algorithm in use (linear or nonlinear). The linear approach (Eq. (2)) provides moderate quality, the nonlinear approach (Eq. (3) and (4)) provides high resolution for the estimate of the largest error.

The error structure is presented by Figs. 4,5, which provide the true error, irremovable uncertainty, linear error estimate, and improved estimate (estimate + irremova-

ICCS Camera Ready Version 2023
To cite this paper please use the final published version:
DOI: 10.1007/978-3-031-36030-5_51

ble uncertainty). One may see that the irremovable uncertainty $b_m = -\frac{1}{n}\sum_j^n \Delta\tilde{\rho}_m^{(j)}$ is the main source of the uncertainty at both the linear and nonlinear estimation of approximation error. Fortunately, it spoils significantly the small errors and leaves safe the great errors. The improved estimate is close to the true error for both linear and nonlinear approaches.

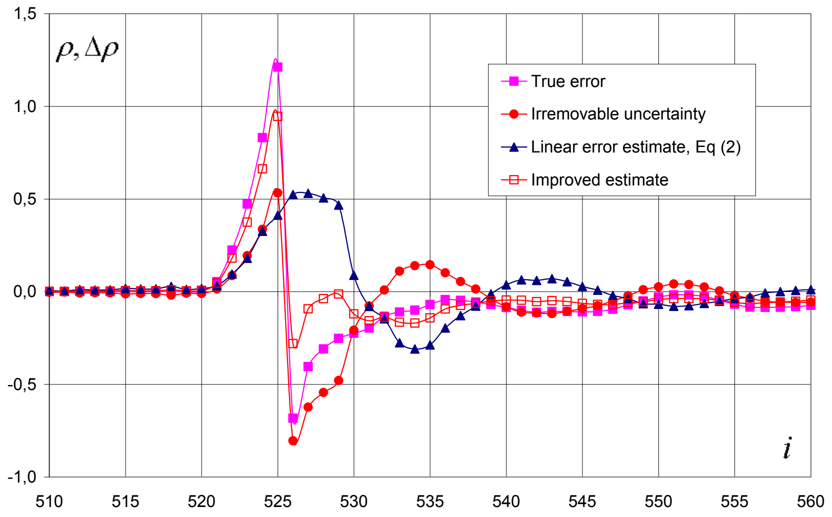

Fig. 4. The errors' structure for solution computed by rCF solver.

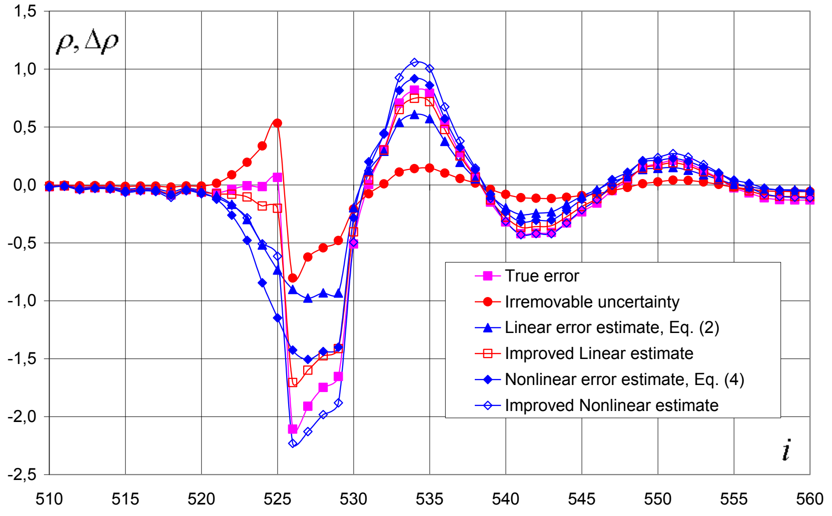

Fig. 5. The errors' structure for solution computed by sF solver

ICCS Camera Ready Version 2023
To cite this paper please use the final published version:
DOI: 10.1007/978-3-031-36030-5_51

Second, the ensemble of rCF,pCF,QGDF solvers is used. The Fig. 6 presents the vectorized density and estimates of errors for rCF based solution. The Fig. 7 presents the analogical information for pCF based solution, Fig. 8 demonstrates QGDF based solution. The results are qualitatively close to previous (Figs. 1-5). The magnitude of the approximation error for solution computed by QGDF is less if compare with solution by sF. By this reason, the error of QGDF based solution is estimated with less accuracy if compare with sF based solution.

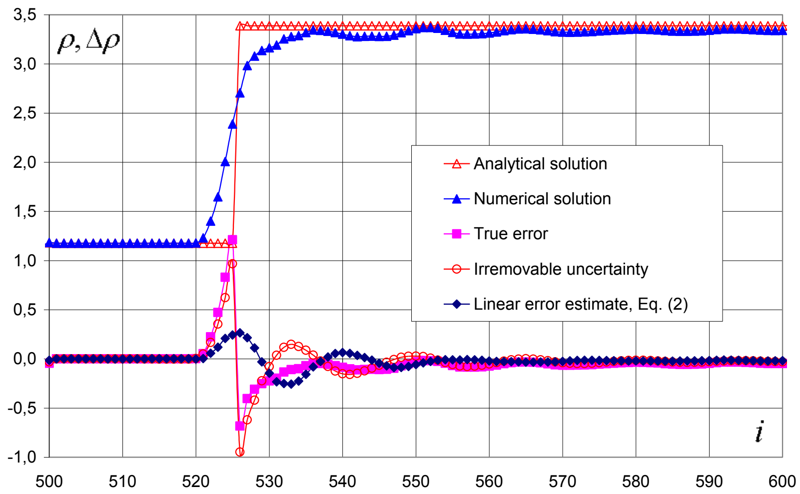

Fig. 6. The vectorized density and density errors for solution computed by rCF solver

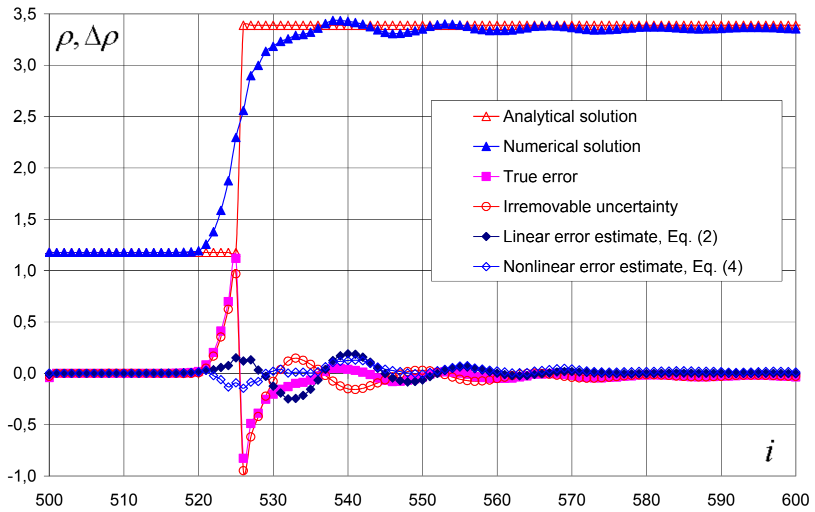

Fig. 7. The vectorized density and density errors for solution computed by pCF solver.

ICCS Camera Ready Version 2023
To cite this paper please use the final published version:
DOI: 10.1007/978-3-031-36030-5_51

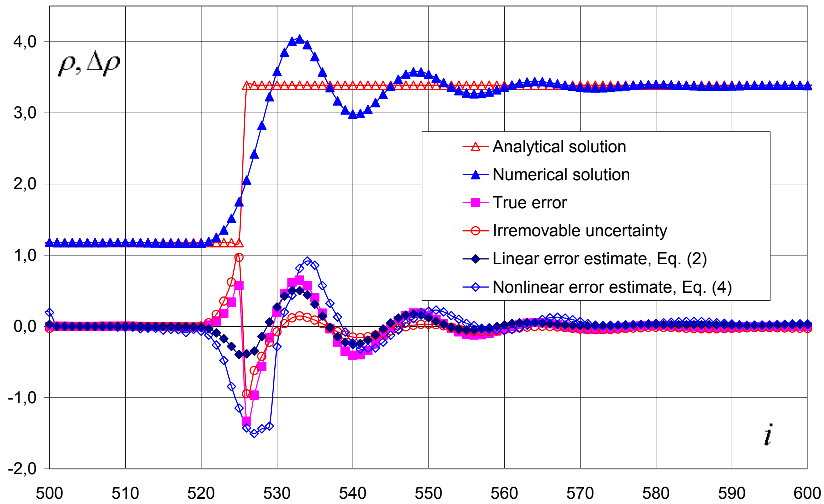

Fig. 8. The vectorized density and density errors for solution computed by QGDF solver.

7 Discussion

The present results demonstrate the feasibility of the precise estimation of the approximation error for the most inaccurate solution from the ensemble of numerical solutions, obtained by different algorithms.

The numerical tests demonstrated drastic difference of the error resolution provided by the linear and nonlinear approaches. The linear approach resolves all errors with the same quality (if abstract from the unremovable uncertainty). The sensitivity of the solution component in the nonlinear case may be estimated from expression $\delta x_i = A_{ij}^{-1}(x)\delta f_j + \delta A_{ij}^{-1}(x) f_j = B_{ij}(x)\delta f_j$ as $|\delta x_i| \le C_i \cdot \|\delta f_j\|$, where $C_i = \|B_{ij}(x)\|$ is the norm of matrix row. So, the sensitivity of different components of the solution may be different and some components of the solution may belong to the nullspace of matrix [26]. The numerical tests demonstrated that the nonlinear approach practically does not resolve small errors, while the great error is resolved with the high accuracy.

At first glance, the numerical solution having a great approximation error can not be valuable. However, in the frame of the ensemble based error estimation [25] such solution enables to generate some hypersphere (with the centre at some precise solution) that contain the true solution. So, the precise estimation of the approximation error is very important, since it justifies the application of the ensemble based method [25] for capture of true solution.

In general, it enables to construct the numerical solution in the sense of Synge [1,2]. At present, the numerical solution is commonly considered to be an element of the sequence converging to the exact solution as the step of discretization decrease. By this reason, the mesh refinement is the key element of the modern CFD practice. Contrary to this approach, Synge stated ([1], p. 97): ***"In general, a limiting process is***

ICCS Camera Ready Version 2023
To cite this paper please use the final published version:
DOI: 10.1007/978-3-031-36030-5_51

not used, and we do not actually find the solution.... But although we do not find it, we learn something about its position, namely, that it is located on a certain hypercircle in function space".

This approach easily enables to estimate the errors of the valuable functionals (using Cauchy–Bunyakovsky–Schwarz inequality) without an adjoint approach. The acceptance of the error magnitude of the functionals used in practices (drag, lift etc.) may serve as a natural criterion for the necessity of the grid refinement.

At present, the domain of applicability of the Singe's approach is limited by equations of special form (Poisson equation, biharmonic equation). In this work, the Synge idea is realized on the basis of ensemble of numerical solutions that relaxes restrictions of Synge method applicability.

8 Conclusion

Due to the presence of irremovable uncertainty, the linear version of the considered ensemble based algorithm enables to estimate the greatest approximation error with the acceptable accuracy, while the errors of more precise solutions are resolved with the lesser quality.

The nonlinear version of the ensemble based algorithm enables the estimation of the greatest approximation error with the higher accuracy (if compare with the linear case), while the errors of more precise solutions are practically not resolved. The precisely resolved component of the error may be detected from the analysis of the distances between numerical solutions and corresponds to the most distant solution.

References

1. Synge J.L., The Hypercircle in Mathematical Physics, CUP, London, 1957
2. Synge J.L., The Hypercircle method, In Studies in Numerical Analysis, Academic Press, London, 1974, p. 201-217
3. Repin, S.I.: A posteriori estimates for partial differential equations. Vol. 4. Walter de Gruyter (2008). https://doi.org/10.1515/9783110203042
4. Roy Ch. J. and Raju A., Estimation of Discretization Errors Using the Method of Nearby Problems. AIAA J. 45(6) (2007) 1232-1243.
5. Richardson, L. F., The Approximate Arithmetical Solution by Finite Differences of Physical Problems Involving Differential Equations with an Application to the Stresses in a Masonry Dam, Transactions of the Royal Society of London, Series A, Vol. 2 10, 1908, pp. 307–357.
6. Banks, J. W., Aslam, T. D.: Richardson Extrapolation for Linearly Degenerate Discontinuities, Journal of Scientific Computing, May 24, 2012 P. 1-15
7. Roy, Ch. J. Grid Convergence Error Analysis for Mixed-Order Numerical Schemes, AIAA Journal, 41(4) (2003) 595-604.
8. Alekseev, A.K., Bondarev, A.E., Kuvshinnikov, A.E.: A Comparison of the Richardson Extrapolation and the Approximation Error Estimation on the Ensemble of Numerical Solutions. ICCS 2021, Lecture Notes in Computer Science, vol. 12747. pp. 554-566. Springer (2021). https://doi.org/10.1007/978-3-030-77980-1_42

ICCS Camera Ready Version 2023
To cite this paper please use the final published version:
DOI: 10.1007/978-3-031-36030-5_51

9. Standard for Verification and Validation in Computational Fluid Dynamics and Heat Transfer, ASME V&V 20-2009, 2009
10. Guide for the Verification and Validation of Computational Fluid Dynamics Simulations, American Institute of Aeronautics and Astronautics, AIAA-G-077-1998, 1998.
11. Alekseev A.K., Bondarev A. E., Kuvshinnikov A. E.: A posteriori error estimation via differences of numerical solutions, ICCS 2020. Lecture Notes in Computer Science (LNCS), vol. 12143, pp. 508–519. Springer, Cham (2020). https://doi.org/10.1007/978-3-030-50436-6_37
12. Alekseev A.K., Bondarev A.E., The Estimation of Approximation Error using Inverse Problem and a Set of Numerical Solutions, Inverse Problems in Science and Engineering. 29 (13), 3360–3376 (2021). https://doi.org/10.1080/17415977.2021.2000604
13. Alekseev, A.K., Bondarev, A.E., Kuvshinnikov, A.E.: On a Nonlinear Approach to Uncertainty Quantification on the Ensemble of Numerical Solutions, ICCS 2022, LNCS 13353, pp. 637–645, 2022.
14. Press W. H., Flannery B. P., Teukolsky S. A., Vetterling W. T., Numerical Recipes in Fortran 77: The Art of scientific computing, Cambridge Univ. Press, 1992
15. Moore, E. H. On the reciprocal of the general algebraic matrix. Bulletin of the American Mathematical Society. 26 *(9): 394–95.* (1920).
16. Penrose, R. A generalized inverse for matrices. Proceedings of the Cambridge Philosophical Society. *51 (3): 406–13.* (1955).
17. Tikhonov, A.N., Arsenin, V.Y.: Solutions of Ill-Posed Problems. Winston and Sons, Washington DC (1977).
18. Alifanov, O.M., Artyukhin, E.A., Rumyantsev S.V.: Extreme Methods for Solving Ill-Posed Problems with Applications to Inverse Heat Transfer Problems. Begell House (1995).
19. OpenFOAM, http://www.openfoam.org.
20. Kurganov, A., Tadmor, E.: New high-resolution central schemes for nonlinear conservation laws and convection-diffusion equations. J. Comput. Phys. 160(1), 241–282 (2000). https://doi.org/10.1006/jcph.2000.6459
21. Greenshields, C., Wellerr, H., Gasparini, L., Reese, J.: Implementation of semi-discrete, non-staggered central schemes in a colocated, polyhedral, finite volume framework, for high-speed viscous flows. Int. J. Numer. Meth. Fluids 63(1), 1–21 (2010). https://doi.org/10.1002/fld.2069
22. Issa, R.: Solution of the implicit discretized fluid flow equations by operator splitting. J. Comput. Phys. 62(1), 40–65 (1986). https://doi.org/10.1016/0021-9991(86)90099-9
23. Kraposhin, M., Bovtrikova, A., Strijhak, S.: Adaptation of Kurganov-Tadmor numerical scheme for applying in combination with the PISO method in numerical simulation of flows in a wide range of Mach numbers. Procedia Computer Science 66, 43–52 (2015). https://doi.org/10.1016/j.procs.2015.11.007
24. Kraposhin, M.V., Smirnova, E.V., Elizarova, T.G., Istomina, M.A.: Development of a new OpenFOAM solver using regularized gas dynamic equations. Computers & Fluids, 166, 163–175 (2018). https://doi.org/10.1016/j.compfluid.2018.02.010
25. Alekseev A.K., Bondarev A. E., Kuvshinnikov A. E., On Uncertainty Quantification via the Ensemble of Independent Numerical Solutions, Journal of Computational Science, 42 (2020), 10114
26. Strang G., The fundamental theorem of linear algebra, American Mathematical Monthly, 100:9, 1993, 848-859.

ICCS Camera Ready Version 2023
To cite this paper please use the final published version:
DOI: 10.1007/978-3-031-36030-5_51